

3D multifrequency abdominal MR elastography using a piezoelectric driver, single-shot wave-field acquisition, and multifrequency dual parameter inversion

Jing Guo¹, Sebastian Hirsch¹, Rolf Reiter¹, Thomas Kroencke¹, Patrick Asbach², Juergen Braun³, and Ingolf Sack¹

¹Department of Radiology, Charite - University Medicine Berlin, Berlin, Germany, ²MVZ CBF Radiologie, Charite - University Medicine Berlin, Berlin, Berlin, Germany, ³Department of Medical Informatics, Charite - University Medicine Berlin, Berlin, Berlin, Germany

Target audience: Radiologists and MR physicists who are interested and working in the field of MR elastography (MRE).

Purpose: To improve the clinical applicability of abdominal MRE [1] and to reduce reconstruction artifacts causing uncertain regions in viscoelasticity maps by introducing a novel 3D multifrequency MRE technique based on a piezoelectric driver, single-shot wave-field acquisition and multifrequency dual parameter inversion. Furthermore, we test the new method on healthy volunteers and patients with ascites regularly challenging the external wave stimulation of the liver.

Methods: *Subjects:* Abdominal MRE was applied to ten healthy volunteers (3 females, age range from 22 to 51 years) and four patients with portal hypertension (2 females, age range from 58 to 75 years, portosystemic pressure gradients of 32, 18, 12, 27 mmHg, respectively). *Experiments:* All experiments were conducted on a 1.5-T MRI scanner equipped with a 12-channel phased array surface coil. Single-shot spin-echo EPI with flow-compensated motion-encoding gradient (MEG) was used for rapid 3D motion field acquisition. Vibration frequencies were 30, 40, 50 and 60 Hz. For each drive frequency, MEG-direction and wave dynamic, 10 adjacent transversal image slices of $2.7 \times 2.7 \times 5 \text{ mm}^3$ resolution were recorded. Data acquisition was split into 12 breath holds of 15 sec each. Total examination time was 6 to 8 min. Further imaging parameters: TR / TE = 182 ms / 54 ms; field of view (FoV), $350 \times 284 \text{ mm}^2$; matrix size 128×104 ; MEG frequency, 50 Hz; MEG amplitude, 30 mT/m. *Data post-processing and multifrequency dual parameter recovery:* Gradient-based unwrapping was performed as proposed by [2]. For reducing noise, numerical derivatives were calculated by 3D gradients according to Anderssen and Hegland [3] using a two-pixel symmetric window in three dimensions. The resulting strain components of the wave field were used to calculate the curl field. To improve the resolution of MRE parameter maps, we employed two separated single-step multifrequency inversion algorithms named multifrequency dual elasto-visco (MDEV) inversion. In short, we start with representing the complex modulus by its magnitude and phase, $G^* = |G^*|(\cos\phi + i\sin\phi)$, introduce this representation into the Helmholtz wave equation (see eq.(9) of [4]) and continue with reconstruction of ϕ by solving $\Delta \mathbf{x}_{mn} \cdot \mathbf{x}_{mn} = -|\Delta \mathbf{x}_{mn}| |\mathbf{x}_{mn}| \cos\phi$ in a least-squares sense. \mathbf{x}_{mn} is composed of real and imaginary parts of the m^{th} -component of the curl wave field at n^{th} -frequency, $c'_m(\omega_n)$ and $c''_m(\omega_n)$, respectively. ϕ is scaled by $2/\pi$ to α which is known from springpot-model based MRE as the powerlaw exponent [5]. As a second parameter, we reconstruct $|G^*|$ by least-squares solution of the magnitude-Helmholtz equation $|G^*| |\Delta c'_m(\omega_n)| = \rho \omega_n^2 |c'_m(\omega_n)|$.

Results: As seen from Fig.2, liver, vessels, fluid-filled ascites, and the spleen are well resolved by $|G^*|$ and α . It is remarkable that areas of larger vessels as inferior vena cava and abdominal aorta are identifiable with low intensity in the $|G^*|$ -map, revealing the low shear modulus of such fluid-filled compartments. Patients have significantly higher α -values ($\alpha = 0.511 \pm 0.060$) compared to healthy volunteers ($\alpha = 0.313 \pm 0.041$, $P = 1.1 \cdot 10^{-5}$), whereas the group-mean shear modulus $|G^*|$ is not altered between our groups (volunteers: $1.44 \pm 0.23 \text{ kPa}$, patients: $1.96 \pm 0.99 \text{ kPa}$, $P = 0.129$). We use the intra-hepatic standard deviations for quantifying heterogeneity. The SD-values are generally lower in healthy volunteers than in patients (SD of $|G^*| = 0.54 \pm 0.09 \text{ kPa}$ [volunteers], SD of $|G^*| = 1.07 \pm 0.61 \text{ kPa}$ [patients], $P = 0.015$; SD of $\alpha = 0.157 \pm 0.026$ [volunteers], SD of $\alpha = 0.217 \pm 0.012$ [patients], $P = 0.001$). In the group of healthy volunteers, both parameters $|G^*|$ and α are higher in the spleen than in the liver ($P = 0.015$ and $6.58 \cdot 10^{-5}$, respectively). In the same group, a significant correlation between splenic and hepatic stiffness ($|G^*|$) exists, as illustrated by Pearson's linear correlation coefficient ($R = 0.8488$, $P = 0.002$) which agrees with literature values [6]. However, no such correlation between splenic and hepatic MRE constants was found for α or for both $|G^*|$ and α in patients.

Discussion: It is a stimulating result that we could resolve hepatic and splenic stiffness by the same scan in all subjects including those with ascites. The higher powerlaw exponent α in the spleen suggests that the spleen has a more strongly cross-linked mechanical structure than the liver. Given that nearly 80% of the spleen is made up of red pulp, which consists of fibrils and connective tissue cells, it is not surprising that splenic α is significantly higher. Our study reproduces the correlation of splenic and hepatic stiffness reported in [6,7]. However, the lack of correlation between splenic and hepatic α suggests that $|G^*|$ in both organs is sensitive to mechanisms which do not alter the inherent tissue architecture such as changing vascular pressure, interstitial fluid accumulation, or strengthening of connective tissue.



Fig.1: Proposed nonmagnetic driver system for abdominal MRE. A close view of the driver which is placed at the end of the patient table is shown in the left image. A carbon fiber rod is mounted to the horizontal lever arm for efficient wave transmission to the transducer mat (shown in the upper right image). The entire setup is shown in the bottom right figure. The vibration direction is indicated by arrows.

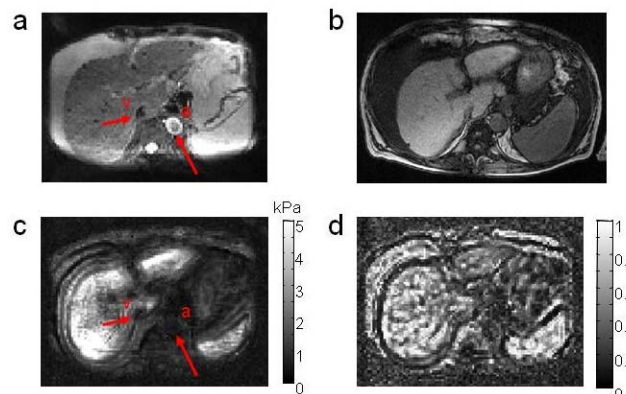


Fig.2: Slice from a 3D-MRE data set of patient with portal hypertension, ascites and fibrosis. Magnitude of the MRE signal (a), T1-weighted anatomical image (b), $|G^*|$ (c) and α (d). Inferior vena cava and descending aorta are pointed by arrows, labeled with "v" and "a", respectively.

Conclusion: 3D multifrequency MRE including nonmagnetic shear wave excitation and least-squares multifrequency inversion was introduced for improving the spatial resolution of abdominal MRE. The proposed method is suitable for the reproducible measurement of spatially resolved viscoelastic parameter maps in liver and spleen with minimized inversion-related artifacts. The piezo-based driver system is easy to handle in clinical examinations.

References: [1] Muthupillai R, Lomas DJ, Rossman PJ, Greenleaf JF, Manduca A, Ehman RL. Magnetic resonance elastography by direct visualization of propagating acoustic strain waves. *Science*. 1995;269:1854–1857. [2] Papazoglou S, Xu C, Hamhaber U, et al. Scatter-based magnetic resonance elastography. *Phys Med Biol*. 2009; 54: 2229-2241. [3] Anderssen RS, Hegland M. For numerical differentiation, dimensionality can be a blessing! *Math Comput*. 1999; 68: 1121-1141. [4] Papazoglou S, Hirsch S, Braun J, Sack I. Multifrequency inversion in magnetic resonance elastography. *Phys Med Biol*. 2012; 57: 2329-2346. [5] Streitberger KJ, Sack I, Krefling D, et al. Brain viscoelasticity alteration in chronic-progressive multiple sclerosis. *PLoS one*. 2012; 7: e29888. [6] Talwalkar JA, Yin M, Venkatesh S, et al. Feasibility of in vivo MR elastographic splenic stiffness measurements in the assessment of portal hypertension. *AJR Am J Roentgenol*. 2009; 193: 122-127. [7] edredal GI, Yin M, McKenzie T, et al. Portal hypertension correlates with splenic stiffness as measured with MR elastography. *J Magn Reson Imaging*. 2011; 34: 79-87.